Astron. Astrophys. 169, 185–188 (1986)

ASTRONOMY AND ASTROPHYSICS

Trapped non-radial oscillation modes in Wolf-Rayet models

R. Scuflaire and A. Noels

Institut d'Astrophysique, Université de Liège, Avenue de Cointe 5, B-4200 Ougrée, Belgium

Received June 2, accepted July 23, 1986

Summary. Computed models of WN stars, evolving with mass loss, go through a phase where non-radial oscillation modes may be trapped in the H-burning shell. We have found that, in a $100\,M_\odot$ sequence, this favours an instability apt to amplify these modes.

Key words: Non-radial oscillations – Wolf-Rayet stars – vibrational instability

1. Introduction

Vreux (1985) and Vreux et al. (1985) have suggested that the variability of emission lines of Wolf-Rayet stars might be due to non-radial pulsations. This behaviour might be common at least among the WN.

Noels and Scuflaire (1986) have then searched a theoretical support to this hypothesis. They have followed the evolution with mass loss of a $100\,M_\odot$ Population I stellar model. This model may represent a Wolf-Rayet star during certain phases of its evolution. These authors have found their models 3 and 4 unstable towards a non-radial $l = 1$ mode [l is the degree of the spherical harmonics used in the description of a non-radial mode, see for instance Boury et al. (1975)]. The unstable modes are sustained by the combustion of hydrogen in a shell. This instability is rather mild and affects a rather short phase of the evolution.

The structure of both these models or, more precisely, the behaviour of the Brunt-Väisälä frequency in the H-burning shell allows the trapping on non-radial modes with moderately high l values. With their large amplitudes in the destabilizing zone, these modes have chances to be unstable. Such unstable modes have already been obtained by Shibahashi and Osaki (1976) for models of 5, 11, 20, and $40\,M_\odot$. They found short-lived vibrational instability for non-radial modes trapped in the nuclear-burning shell. In Sect. 2, we examine the conditions which favour the existence of trapped modes. In the next section, these considerations are applied to the models of the evolutionary sequence. Then we report the results of our computations of vibrational stability.

2. Trapped modes

Adiabatic non-radial oscillation modes of a star are described by functions of the form

$$f(r)\,Y_{lm}(\theta,\phi)\,e^{-i\sigma t},$$

where Y_{lm} is a spherical harmonics. The function $f(r)$, which gives the amplitude in the shell located at a distance r from the centre of the star, can have an oscillatory behaviour (in the r variable) only if the angular frequency σ of the mode is greater or lesser than both cut-off frequencies σ_a (acoustic cut-off frequency) and σ_g (gravity cut-off frequency). In the first case, locally, the given mode behaves as an acoustic wave (pressure effects dominate, p-mode). In the second case, it behaves as a gravity wave (buoyancy effects dominate, g-mode) (Scuflaire, 1974a, b).

The local acoustic cut-off frequency is given by

$$\sigma_a = \frac{\sqrt{l(l+1)}\,c}{r},$$

where c is the local sound speed.

The gravity cut-off frequency is the Brunt-Väisälä frequency

$$\sigma_g = \sqrt{-Ag}$$

with

$$A = \frac{d\ln\varrho}{dr} - \frac{1}{\Gamma_1}\frac{d\ln P}{dr}.$$

In the convective zone, σ_g is imaginary and a dynamically stable mode (i.e. with real σ) can locally oscillate only if $\sigma > \sigma_a$.

When σ is locally between both cut-off frequencies, the amplitude $f(r)$ has an exponential behaviour, but it is generally not possible to state if it is increasing or decreasing. One uses to say that the given mode is locally evanescent.

A necessary condition (but not always a sufficient one) for modes to be trapped is to have a narrow oscillatory region surrounded by two evanescent zones.

Nuclear burning has a destabilizing (amplifying) effect on oscillation modes whereas transfer phenomena most often contribute to their stabilization (damping). Modes trapped in the hydrogen-burning shell would have good chances of being unstable, as their large amplitude in this zone would increase the relative importance of the destabilizing terms (Eq. (1) of Noels and Scuflaire, 1986).

3. Models

Table 1 of Noels and Scuflaire (1986) gives the properties of the models of the evolutionary sequence they have computed. Our Table 1 is drawn out of it and shows the properties of models 3 and 4. These models have structures which favour trapping of modes in the hydrogen burning shell. Figures 1 and 2 give for both models

Send offprint requests to: R. Scuflaire

Table 1. The table gives a few properties of the models. Usual notations have been used. t is the age of the model

	Model 3	Model 4
$M/M_\odot$	41.02	40.94
$L/L_\odot$	1.335 (6)	1.503 (6)
$R/R_\odot$	4.806	6.155
T_e(K)	90033	82111
T_c(K)	1.261 (8)	1.717 (8)
ϱ_c(g cm^{-3})	57.46	152.7
$\varrho_c/\bar{\varrho}$	110.4	617.5
t(yr)	2.718 (6)	2.720 (6)

the behaviour of the cut-off frequencies. In both models, σ_g has a well marked maximum. For moderately high values of l, this maximum is below the acoustic cut-off frequency σ_a. Hence, a range of frequency exist, in which a non-radial mode has an oscillatory behaviour in the hydrogen burning shell and an evanescent behaviour outside of it. Figures 1 and 2 show that modes could be trapped if their frequencies are lower than $1.7\ 10^{-3}\,s^{-1}$ for model 3 and $3.9\ 10^{-3}\,s^{-1}$ for model 4.

4. Adiabatic modes

A few adiabatic non-radial modes have been computed for $l=5$ and 10 and classified in the usual way (Scuflaire, 1974b; Osaki,

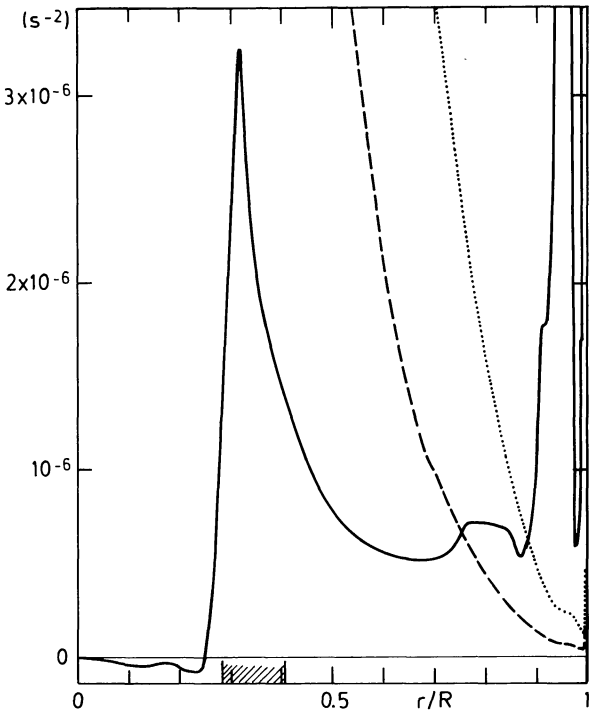

Fig. 1. Model 3. The solid line gives σ_g^2, the dashed line σ_a^2 for $l=5$ and the dotted line σ_a^2 for $l=10$, as a function of the radius r. The hatchings mark the hydrogen burning shell

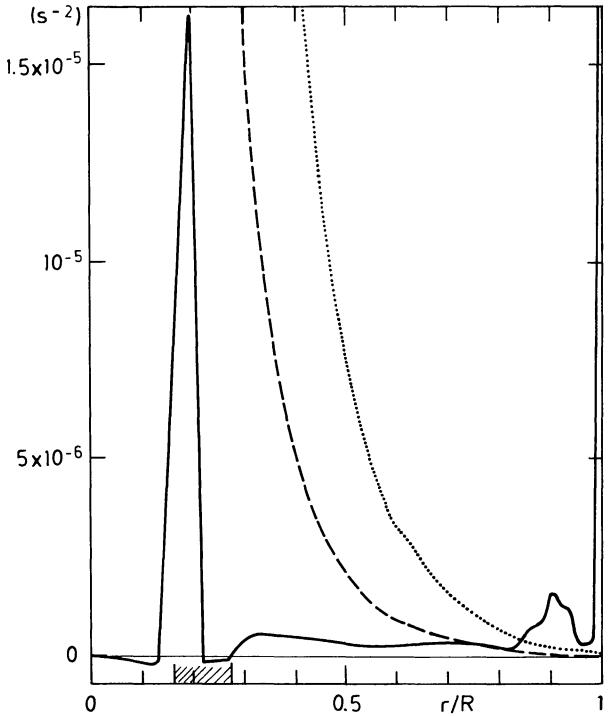

Fig. 2. Model 4. The solid line gives σ_g^2, the dashed line σ_a^2 for $l=5$ and the dotted line σ_a^2 for $l=10$, as a function of the radius r. The hatchings mark the hydrogen burning shell

Table 2. Model 3. The table gives, for the computed modes, the angular frequency σ, the period τ, the damping coefficient σ' and the damping time τ'. A minus sign means amplification

	ℓ = 5				ℓ = 10			
	σ/s^{-1}	τ/hour	σ'/s^{-1}	τ'/year	σ/s^{-1}	τ/hour	σ'/s^{-1}	τ'/year
g_6	3.352(-4)	5.207	3.049(-9)	1.039(1)	5.644(-4)	3.092	4.444(-9)	7.130
g_5	3.869(-4)	4.510	3.369(-9)	9.406	6.359(-4)	2.745	8.176(-9)	3.876
g_4	4.373(-4)	3.991	2.591(-9)	1.223(1)	6.793(-4)	2.569	8.262(-9)	3.835
g_3	5.184(-4)	3.367	5.057(-10)	6.266(1)	7.706(-4)	2.265	4.248(-10)	7.459(1)
g_2	6.929(-4)	2.519	6.632(-11)	4.778(2)	9.568(-4)	1.824	5.053(-11)	6.271(2)
g_1	1.080(-3)	1.616	3.343(-12)	9.479(3)	1.312(-3)	1.330	-1.117(-11)	-2.837(3)
f	1.390(-3)	1.256	3.992(-8)	7.938(-1)	1.604(-3)	1.088	7.871(-8)	4.026(-1)
p_1	1.817(-3)	0.9607	5.706(-7)	5.553(-2)	2.117(-3)	0.8244	1.566(-6)	2.023(-2)
p_2	2.244(-3)	0.7776	2.445(-6)	1.296(-2)	2.509(-3)	0.6955	2.404(-6)	1.318(-2)
p_3	2.572(-3)	0.6786	1.042(-6)	3.041(-2)	2.811(-3)	0.6208	1.759(-6)	1.801(-2)
p_4	2.868(-3)	0.6086	2.562(-6)	1.237(-2)	3.202(-3)	0.5451	1.708(-6)	1.855(-2)
p_5	3.236(-3)	0.5393	1.298(-6)	2.441(-2)	3.621(-3)	0.4820	1.980(-6)	1.600(-2)
p_6	3.633(-3)	0.4804	1.262(-6)	2.511(-2)	4.030(-3)	0.4331	3.549(-6)	9.161(-3)
p_7	4.019(-3)	0.4343	3.273(-6)	9.682(-3)	4.436(-3)	0.3934	1.653(-6)	1.917(-2)

Table 3. Model 4. The table gives, for the computed modes, the angular frequency σ, the period τ, the damping coefficient σ' and the damping time τ'. A minus sign means amplification

	$\ell = 5$				$\ell = 10$			
	σ/s^{-1}	τ/hour	σ'/s^{-1}	τ'/year	σ/s^{-1}	τ/hour	σ'/s^{-1}	τ'/year
g_6	5.521(-4)	3.161	1.608(-10)	1.971(2)	8.536(-4)	2.045	1.766(-10)	1.794(2)
g_5	5.860(-4)	2.978	1.020(-10)	3.107(2)	1.009(-3)	1.730	1.086(-10)	2.918(2)
g_4	7.183(-4)	2.430	3.964(-11)	7.994(2)	1.140(-3)	1.531	2.807(-7)	1.129(-1)
g_3	8.838(-4)	1.836	9.256(-11)	3.423(2)	1.221(-3)	1.429	6.161(-11)	5.143(2)
g_2	9.965(-4)	1.751	1.507(-7)	2.103(-1)	1.399(-3)	1.247	3.881(-6)	8.165(-3)
g_1	1.286(-3)	1.358	2.320(-6)	1.366(-2)	1.541(-3)	1.133	3.072(-11)	1.032(3)
f	1.412(-3)	1.236	4.152(-9)	7.632	1.606(-3)	1.087	1.641(-6)	1.931(-2)
p_1	1.440(-3)	1.212	2.387(-7)	1.328(-1)	1.894(-3)	0.9216	7.324(-7)	4.327(-2)
p_2	1.673(-3)	1.043	3.839(-6)	8.254(-3)	2.082(-3)	0.8382	3.169(-12)	9.999(3)
p_3	1.936(-3)	0.9017	4.235(-7)	7.482(-2)	2.168(-3)	0.8051	1.795(-6)	1.765(-2)
p_4	2.200(-3)	0.7932	2.251(-6)	1.408(-2)	2.446(-3)	0.7136	1.497(-6)	2.117(-2)
p_5	2.466(-3)	0.7079	1.089(-6)	2.910(-2)	2.739(-3)	0.6371	1.978(-6)	1.602(-2)
p_6	2.592(-3)	0.6734	3.976(-8)	7.970(-1)	3.037(-3)	0.5746	1.339(-6)	2.367(-2)
p_7	2.749(-3)	0.6348	2.062(-6)	1.537(-2)	3.128(-3)	0.5580	-8.345(-12)	-3.797(3)
p_8	3.035(-3)	0.5750	1.187(-6)	2.670(-2)	3.337(-3)	0.5231	2.262(-6)	1.401(-2)

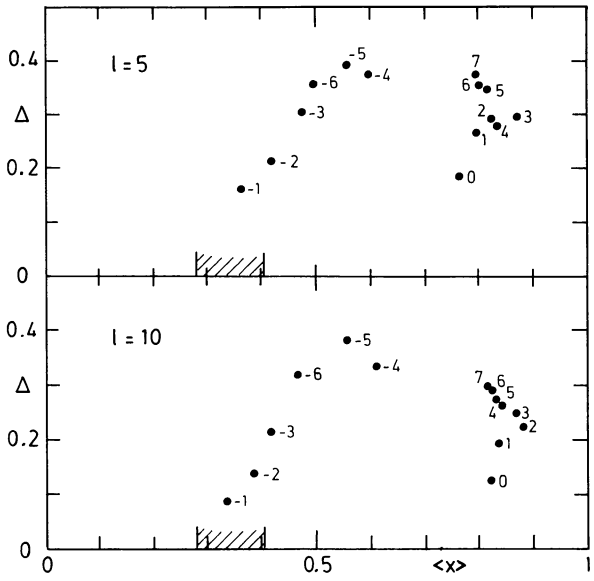

Fig. 3. Model 3. The modes from g_6 to p_7 of $l=5$ and $l=10$ are plotted in the $\langle x\rangle$, Δ plane. Positive numbers indicate p modes, negative numbers g modes and zero the f mode. Hatchings mark the hydrogen burning shell

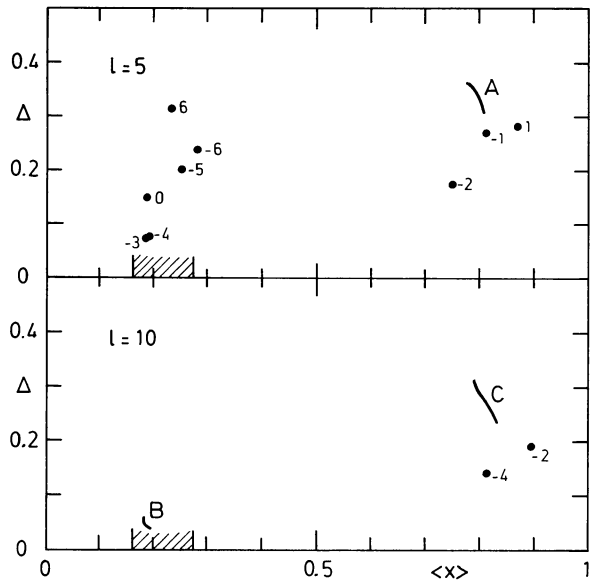

Fig. 4. Model 4. The modes from g_6 to p_7 of $l=5$ and 10 have been plotted in the $\langle x\rangle$, Δ plane. Positive numbers indicate p modes, negative numbers g modes and zero the f mode. Hatchings mark the hydrogen burning shell, A, B, and C indicate families of modes, too close to each other to be separately plotted. A: p_2, p_3, p_4, p_5, and p_7; B: g_6, g_5, g_3, g_1, p_2, and p_7; C: f, p_1, p_3, p_4, p_5, and p_6

1975). Contrary to the case where $l=1$, we have met no difficulty in the identification of the computed modes. This is due to the fact that when l is not too low, Cowling's approximation becomes better. The angular frequencies σ and the periods $\tau = 2\pi/\sigma$ are given in Tables 2 and 3.

Let f be any variable defined at each point of the star. For a given mode of oscillation, let ξ be the modulus of the displacement. We define the mean of f weighted by the kinetic energy of the mode by

$$\langle f\rangle = \frac{\int \varrho \xi^2 f\, dV}{\int \varrho \xi^2\, dV}.$$

In order to characterize globally each mode, we have used two indices $\langle x\rangle$ and Δ defined by Scuflaire (1980).
$x = r/R$ (R is the radius of the star)

$$\Delta = 2\sqrt{\langle (x - \langle x\rangle)^2\rangle}.$$

The first index localizes the mode in the star and the second one measures its spread. For a perfectly trapped mode, Δ would be zero. As it is defined, its maximum value is 1. Figures 3 and 4 show the positions of the computed modes in the $\langle x\rangle$, Δ plane for both models.

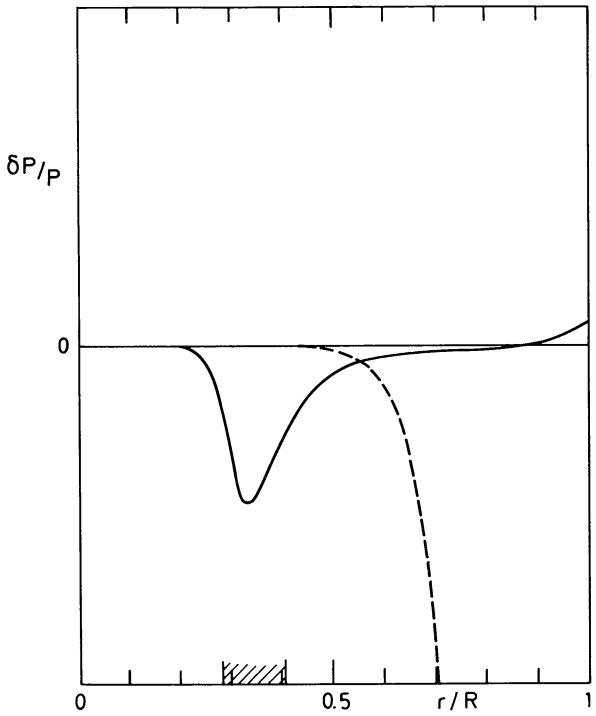

Fig. 5. Model 3. Relative variation of the pressure $\delta P/P$, on an arbitrary scale, for modes g_1 (solid line) and f (dashed line) of $l=10$

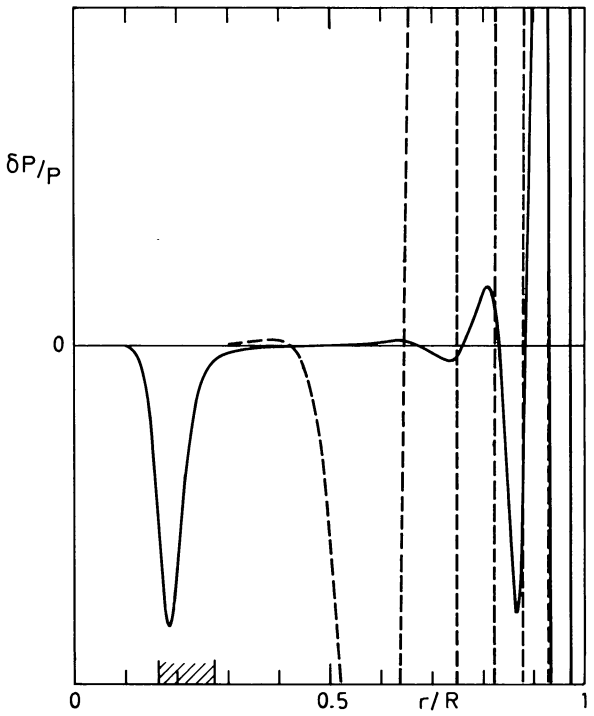

Fig. 6. Model 4. Relative variation of the pressure $\delta P/P$, on an arbitrary scale, for modes p_7 (solid line) and p_6 (dashed line) of $l=10$

For model 3, Fig. 3 shows the difference of behaviour between g and p modes. The properties of the modes evolve regularly with the number of the mode. There is no very well trapped mode. Nevertheless, the first g-modes are localized in the hydrogen burning shell and their spread is not too large. Thus they are good candidates for a vibrational instability.

For model 4, Fig. 4 shows the existence of a whole family of trapped modes. For $l=5$, the modes concerned are g_6, g_5, g_4, g_3, f, and p_6. For $l=10$ they are g_6, g_5, g_3, g_1, p_2, and p_7. The frequencies of these modes are in the range predicted from the examination of Fig. 2.

Figures 5 and 6 show, for both models, two consecutive modes, with neighbouring frequencies but with completely different behaviour. This difference is clearly shown in the $\langle x\rangle$, Δ plane. This plane appears to be a good tool to detect the candidates to a vibrational instability.

5. Vibrational stability

Owing to the non adiabatic phenomena, the modes undergo generally a damping, but sometimes they are amplified. The radiative transfer generally contributes to their damping, whereas nuclear burning has an opposite effect. The net result depends on the balance between those terms. The damping is described by a factor $e^{-\sigma' t}$. Damping is characterized by $\sigma' > 0$ and amplification (i.e. vibrational instability) corresponds to $\sigma' < 0$. The e-folding time τ' is defined by $\tau' = 1/\sigma'$.

Tables 2 and 3 give σ' and τ' for the computed modes. These tables and Figs. 3 and 4 show that for modes favourably located in the $\langle x\rangle, \Delta$ plane, the damping is lower than for other modes. Among them, we have find an unstable mode in each model. The amplification times of these modes are of a few thousand years.

6. Conclusion

The instability we have found in this work is rather mild. The duration of the evolutionary phase during which it is present is only a few times the characteristic time of amplification. Thus the excitation of these modes by the burning of hydrogen in a shell is probably not sufficient to explain any observed variability in this type of star although the pulsation periods for some marginally stable modes lie in the observed range of the order of a few hours. However, if other (presently unknown) destabilizing mechanisms are present, the unstable and marginally stable modes found in this work would become good candidates to explain the observed variability in WN stars.

References

Boury, A., Gabriel, M., Noels, A., Scuflaire, R., Ledoux, P.: 1975, *Astron. Astrophys.* **41**, 279
Noels, A., Scuflaire, R.: 1986, *Astron. Astrophys.* **161**, 125
Osaki, Y.: 1975, *Publ. Astron. Soc. Japan* **27**, 237
Scuflaire, R.: 1974a, *Astron. Astrophys.* **31**, 185
Scuflaire, R.: 1974b, *Astron. Astrophys.* **36**, 107
Scuflaire, R.: 1980, *Bull. Soc. Roy. Sci. Liège* **49**, 164
Shibahashi, H., Osaki, Y.: 1976, *Publ. Astron. Soc. Japan* **28**, 533
Vreux, J.M.: 1985, *Publ. Astron. Soc. Pacific* **97**, 274
Vreux, J.M., Andrillat, Y., Gosset, E.: 1985, *Astron. Astrophys.* **149**, 337